Molecular Cell
Review

Gymnastics of Molecular Chaperones

Matthias P. Mayer[1,*]
[1]Zentrum für Molekulare Biologie der Universität Heidelberg (ZMBH), DKFZ-ZMBH-Allianz, Im Neuenheimer Feld 282, 69120 Heidelberg, Germany
*Correspondence: m.mayer@zmbh.uni-heidelberg.de
DOI 10.1016/j.molcel.2010.07.012

Molecular chaperones assist folding processes and conformational changes in many proteins. In order to do so, they progress through complex conformational cycles themselves. In this review, I discuss the diverse conformational dynamics of the ATP-dependent chaperones of the Hsp60, Hsp70, Hsp90, and Hsp100 families.

Introduction

Movements in proteins can be observed at different structural levels. In addition to atom vibrations, structural units like random coil regions, secondary structure elements, subdomains, and domains change their conformation in a dynamic manner. (Impressive examples for conformational changes in proteins can be found on The Yale Morph Server [http://molmovdb.org/cgi-bin/movie.cgi].) To elucidate such conformational changes, it is often necessary to use a host of different methods. X-ray crystallography provides a rather static view unless alternative conformations of a protein can be crystallized. Electron microscopy (EM) is especially useful for visualizing alternative subunit and domain orientations in large protein complexes. Small-angle X-ray scattering (SAXS) reports on the overall shape of large proteins at low resolution. NMR is the only method that gives truly dynamic pictures at atomic resolution, but is mostly limited to smaller proteins. Hydrogen-^{1}H/^{2}H-exchange (HX) in combination with NMR or mass spectrometry (MS) reports on inherent and induced flexibility in secondary structure. Fluorescence spectroscopy and crosslinking give additional information on changes in the environment or the proximity of structural elements.

Conformational flexibility and rigid body domain movements are the basis for enzymatic catalysis and allosteric regulation (Henzler-Wildman and Kern, 2007). The necessity for flexibility and conformational changes may be one of the reasons why most proteins adapted to a rather narrow temperature range and tend to misfold under heat shock or other environmental stress conditions. To counteract misfolding and the appearance of toxic protein aggregates, molecular chaperones evolved. Chaperones also assist nascent polypeptides in de novo folding and unfold them for degradation by proteolytic machines. They even regulate the conformation of certain natively folded proteins (Picard, 2002; Rodriguez et al., 2008). To fulfill their tasks, chaperones themselves must be structurally dynamic. The elucidation of these conformational changes was a major focus of chaperone research in the last decade, and much progress has been made in recent years. Although ATP-independent chaperones like the small heat shock proteins or Hsp33 also show conformational changes induced by heat or oxidative stress (Franzmann et al., 2008; Janda et al., 2004), in this review I concentrate on the ATP-dependent chaperones of the Hsp60, Hsp70, Hsp90, and Hsp100 families, which in general affect the conformation of their substrates more strongly, e.g., by refolding misfolded and aggregated proteins, by activating inactive species, or by completely unfolding proteins for degradation.

Hsp60s: Dynamics of a Folding Chamber

Hsp60s, also called chaperonins, are found in all domains of life and are large cylindrical oligomers consisting of two rings arranged back to back. Each ring contains a central cavity in which nonnative proteins are encapsulated in an ATP-dependent process for folding into the native state (Frydman, 2001; Horwich et al., 2007). Chaperonin subunits are built up of three domains: the equatorial domain, which contains the nucleotide-binding site and makes the interring contacts; the intermediate domain; and the apical domain, which contains most of the substrate-interacting residues.

Chaperonins are divided into two groups of common evolutionary origin: group I chaperonins are mostly found in prokaryotes, mitochondria, and plastids and group II chaperonins in archaea and the eukaryotic cytosol (Gutsche et al., 1999; Spiess et al., 2004). Group I chaperonins, such as *E. coli* GroEL, are homo-oligomers with seven 57 kDa subunits per ring (Figure 1A), and the two rings contact each other in a 2:1 subunit arrangement, i.e., one subunit of one ring interacts with two subunits in the other. Group II chaperonins, such as TRiC/CCT in the eukaryotic cytosol or the thermosome in archaea, are homo- or hetero-oligomers with eight or nine subunits of 57–61 kDa per ring, and their rings are exactly in register with 1:1 interring subunit contacts. For refolding of misfolded proteins, group I chaperonins cooperate with a homoheptameric cochaperone of 10 kDa subunits (GroES in *E. coli*), which closes the folding chamber like a lid by interacting with the apical domains. In contrast, group II chaperonins do not cooperate with a lid-forming cochaperone but instead have an insertion in the apical domain, which functions as a built-in lid.

The chaperone cycle of chaperonins has been worked out best for *E. coli* GroEL. Nonnative substrates smaller than 60 kDa bind to the interior of one of the two GroEL rings through hydrophobic interactions with several of the seven subunits. ATP binding to the substrate containing *cis*-ring allows GroES binding and enclosure of the substrate. ATP is hydrolyzed with a half-life of 10 s (Horwich et al., 2007). ATP and GroES binding to the *trans*-ring trigger GroES and ADP dissociation from the *cis*-ring and substrate release. Substrates that failed to fold into the

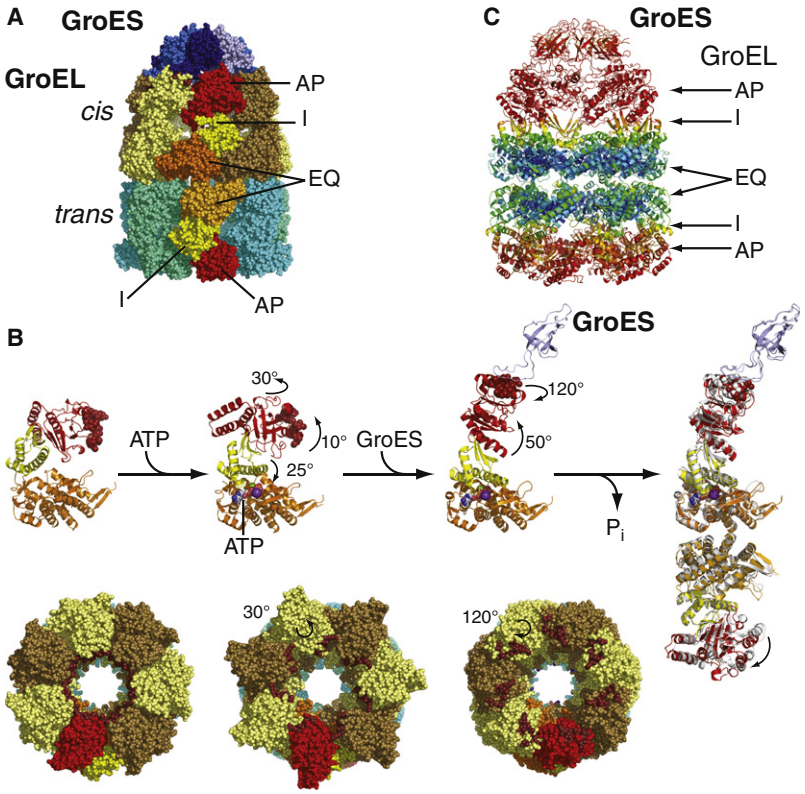

Figure 1. Structure and Conformational Changes of the Group I Chaperonin GroEL-GroES

(A) Sphere representation of the structure of GroEL in complex with GroES and seven ATP bound to the *cis*-ring (PDB entry code 2C7C): GroES subunits in shades of blue; GroEL subunits in brown and yellow (*cis*-ring) and cyan and green-cyan (*trans*-ring); for one subunit in each ring, equatorial (EQ), intermediate (I), and apical domain (AP) are colored in orange, yellow, and red, respectively.

(B) Conformational changes upon ATP binding and hydrolysis. Upper panel shows secondary structure representation for a single GroEL subunit of the *cis*-ring with domains colored in orange, yellow, and red as in A) (PDB entry codes 1AON, 2C7E, 2C7C, 2C7D). For the ADP state, one subunit of the *cis*- and one of the *trans*-ring are shown and overlaid on the ATP + GroES structure in light gray. Hydrophobic residues in the apical domain suspected to interact with substrates are shown as dark red spheres. Lower panel shows sphere representation of the GroEL *cis*-ring in top view with GroES removed in the last image. Substrate-interacting residues are shown in dark red.

(C) Crystal structure of GroEL in complex with GroES and seven ADP colored according to the crystallographic b-factor (blue, low b-factor; red, high b-factor; PDB entry code 1AON). Structural representations were created in PyMOL (http://www.pymol.org).

native state are rebound rapidly, while folded substrates no longer expose hydrophobic residues necessary for binding. ATP binding by GroEL is cooperative within one ring and anti-cooperative between rings. This allows alternate folding in the two chambers: substrate enclosure in one ring leads to substrate release in the other (Yifrach and Horovitz, 1995). A similar nested cooperativity was also proposed for the thermosome, indicating that both groups of chaperonins can act as two-stroke machines (Bigotti and Clarke, 2005; Kafri et al., 2001).

The Conformational Cycle of the GroEL-GroES Machinery

Several crystal structures and extensive high resolution cryo-EM data have elucidated many conformational changes that occur during the ATPase cycle of *E. coli* GroEL (Braig et al., 1994; Ranson et al., 2001, 2006; Xu et al., 1997), the homo-oligomeric group II chaperonin of *Methanococcus maripaludis* (Clare et al., 2008; Zhang et al., 2010), and the hetero-oligomeric mammalian CCT (Booth et al., 2008). In the nucleotide-free state, the tip of the apical domain of GroEL faces the interior of the ring, exposing hydrophobic residues for interaction with misfolded substrates (Figure 1B). Upon ATP binding, the intermediate domain rotates 25° toward the equatorial domain and closes the ATP-binding pocket. The apical domain rotates about 30° counterclockwise and away from the equatorial domain by 10° (Ranson et al., 2001). Interaction with GroES leads to a further upward rotation of 50° and a 120° clockwise rotation of the apical domain (Ranson et al., 2006; Xu et al., 1997). These pivoting movements of the apical domain lead to an enlargement of the folding chamber and to a change in its character: hydrophobic residues, which bind nonnative substrates in the nucleotide-free state, are buried, and the inner wall of the chamber is largely hydrophilic, with many negatively charged residues. (Movies illustrating the dynamics of the folding chamber by connecting the different conformational states elucidated by cryo-EM can be found on Helen Saibil's homepage [http://people.cryst.bbk.ac.uk/~ubcg16z/chaperone.html].) ATP hydrolysis in the *cis*-ring is the slowest step of the ATPase cycle, with a half-life of ca. 10 s, and is therefore considered to be a timer for the folding reaction. It does not induce major conformational changes in the *cis*-ring but weakens the interaction with GroES. In the *trans*-ring, significant conformational changes are induced in all three domains (Ranson et al., 2006). The equatorial domain of the *trans*-ring rotates, leading to a tightening of interring contacts and an expansion of the whole *trans*-ring. In this way, the apical domains of the *trans*-ring tilt outward, away from the equatorial domain and into a position more suitable for catching misfolded proteins or folding intermediates. ATP binding to the *trans*-ring has a profound influence on the *cis*-ring: it induces GroES and substrate release and an upward movement of the intermediate domain with a concomitant inward rotation of the apical domain. This opens the nucleotide-binding pocket in the *cis*-ring, and ADP is released, returning this GroEL ring to the ground state. The large conformational movements of GroEL subunits are envisioned as rigid body movements, with intermediate and apical domains pivoting around defined hinge regions. Interestingly, the b-factor of the crystal structures of the GroEL-GroES complex is low for the equatorial domain but very high for the intermediate and apical domains on both the GroES-free and the GroES-bound sides of the asymmetric complex (Figure 1C). This may indicate a relatively high variance in the domain orientations of

the intermediate and apical domains, but it may also indicate intrinsic flexibility.

Conformational Changes in Group II Chaperonins

For group II chaperonins, progression through the ATPase cycle is also accompanied by massive conformational changes, which have been best analyzed for the chaperonin of *Methanococcus maripaludis* (Mm-Cpn) (Clare et al., 2008; Zhang et al., 2010). In the nucleotide-free state, Mm-Cpn resembles an open cage-like cylinder with intersubunit contacts only in the equatorial domain and separated, rather flexible intermediate and apical domains, reminiscent of tentacles fishing for a catch (Figure 2A). This conformation contrasts the situation in GroEL, where intersubunit contacts are found between all three domains. Upon ATP binding to Mm-Cpn and ATP hydrolysis, the equatorial domains rotate approximately 40° around the interring contact residues. As a consequence, the chamber facing parts of the equatorial domains of the two rings approach each other by approximately 18 Å, and the intermediate and apical domains close the folding chamber through a sideways twisting motion, resulting extensive intersubunit contacts (Figures 2B and 2C). The built-in lid in the apical domain, which is largely unstructured in the open conformation, forms an α helix loop structure and closes the opening of the folding chamber in an iris-like movement (Booth et al., 2008; Zhang et al., 2010). Asymmetric half-closed structures of the Mm-Cpn have also been observed (Clare et al., 2008).

Two major differences are observed between group I and group II chaperonins: (1) In group I chaperonins, closing of the folding chamber is induced by ATP and GroES binding, while ATP hydrolysis is necessary for group II chaperonin closing (Meyer et al., 2003); (2) ATP and GroES binding leads to an expansion of the folding chamber in group I chaperonins, while ATP hydrolysis in group II chaperonins reduces the volume of the folding chamber.

How these conformational changes allow refolding of nonnative proteins is still debated (Hartl and Hayer-Hartl, 2009; Horwich et al., 2009). Prevention of aggregation by encapsulation is certainly an important aspect and is commonly accepted. It has also been proposed that chaperonins induce global unfolding in substrates bound to several subunits during the conformational changes, assist refolding by restricting the conformational space available for the unfolded polypeptide, and alter the energy landscape for the folding process (Lin et al., 2008; Lin and Rye, 2004; Sharma et al., 2008; Shtilerman et al., 1999).

Hsp70: Conformational Dynamics Regulating Substrate Binding

The Hsp70 chaperones, which are essential in all eukaryotes, assist a large number of protein folding processes, including de novo folding of polypeptides, refolding of misfolded proteins, solubilization of protein aggregates, degradation of proteins, translocation of proteins across membranes, assembly and disassembly of oligomeric complexes, and the regulation of stability and activity of certain natively folded proteins (Mayer and Bukau, 2005; Meimaridou et al., 2009).

What is it that makes Hsp70s such versatile utensils in the cellular chaperone toolbox? In contrast to Hsp60s, which

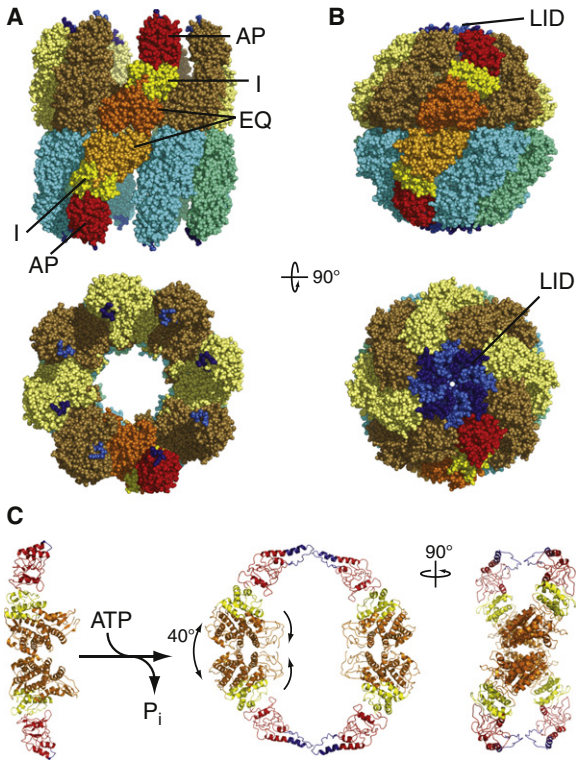

Figure 2. Structure and Conformational Changes of the Group II Chaperonin

(A) Sphere representation of the cryo-EM structure of the *M. maripaludis* chaperonin in the nucleotide-free state, with the built-in lid deleted, is colored as GroEL in Figure 1 (PDB entry code 3IYF). The position of the built-in lid is indicated in blue.

(B) Sphere representation of the cryo-EM structure of the *M. maripaludis* chaperonin in the ATP-bound state. Built-in lid is colored in blue.

(C) Conformational changes upon ATP binding shown for individual subunits in secondary structure representation.

enclose their substrates either entirely or in part, Hsp70s bind a short segment of their substrate polypeptides in their C-terminal substrate-binding domain (SBD). Thus, Hsp70s act locally, and their activity is not limited by the size of their substrates. The interaction with substrates is regulated by the nucleotide status of the N-terminal nucleotide-binding domain (NBD) (Figure 3A). In the ATP-bound state, association and dissociation rates for substrates are high, but affinity for substrates is low. In the ADP-bound and nucleotide-free states, affinity for substrates is high, but substrate exchange rates are low. The basal ATPase rate of Hsp70s is very low but is stimulated by the synergistic action of the substrate and a cochaperone of the family of J-domain proteins (Hsp40). In this way, J-domain proteins couple substrate binding to ATP hydrolysis and to the transition from the low-affinity to the high-affinity state. After formation of the high-affinity Hsp70-substrate complex, ADP dissociation is rate limiting for substrate release at physiological concentrations of ATP. Several different families of nucleotide exchange factors, including the Hsp110 and Hsp170 families, which are close relatives of Hsp70s, accelerate ADP release.

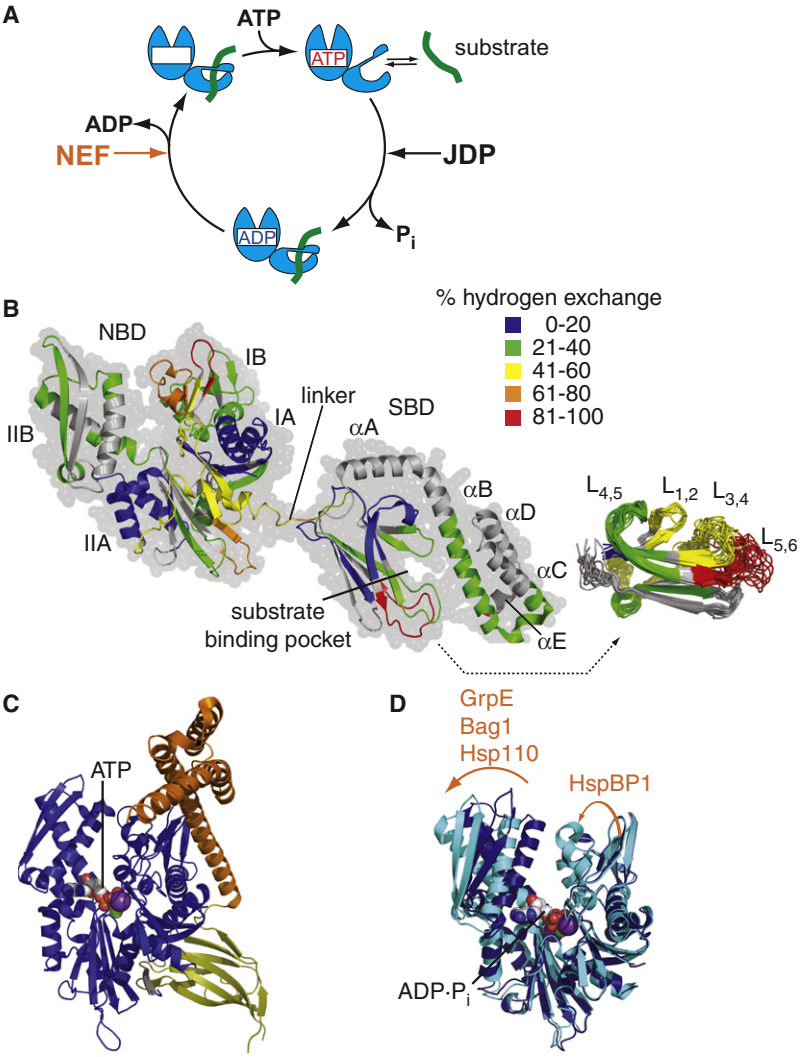

Figure 3. Conformational Dynamics of Hsp70s

(A) ATPase cycle of Hsp70 chaperones regulated by J-domain proteins (JDP) and nucleotide exchange factors (NEF).

(B) Left, overlay of sphere and secondary structure representation of the *E. coli* Hsp70 DnaK determined by NMR residual dipolar coupling (PDB entry code 2KHO) colored according to percent hydrogen exchange in the nucleotide-free protein after 30 s in D_2O, as indicated. Right, NMR structure of the β sheet domain of DnaK colored according to percent hydrogen exchange into the ATP-bound full-length protein after 30 s in D_2O, as indicated.

(C) Crystal structure of the yeast Hsp110 Sse1 (PDB entry code 2QXL). NBD, blue; β sheet subdomain of SBD, yellow; α-helical subdomain of SBD, orange.

(D) Overlay of the crystal structures of bovine Hsc70 NBD in the absence (blue) and presence (cyan) of the Bag domain of Bag1 (PDB entry codes 1HPM and 1HX1). Orange arrows indicate conformational changes induced by the different nucleotide exchange factors.

Dynamics of the SBD

The SBD of Hsp70s is composed of a 25 kDa β sheet subdomain and a 10 kDa helical subdomain (Zhu et al., 1996) (Figure 3B). The β sheet subdomain is built of a sandwich of two twisted four-stranded β sheets with upward protruding loops, which enclose the peptide backbone of the substrate. The helical subdomain consists of five helices, with helices A and B packed against two sides of the β sheet subdomain, stabilizing the inner loops $L_{1,2}$ and $L_{4,5}$. In addition, helix B forms a salt bridge and several hydrogen bonds to the outer Loops $L_{3,4}$ and $L_{5,6}$, the so-called latch, thereby closing the substrate-binding pocket like a lid. Helices C through E, together with the distal part of helix B, form a second hydrophobic core. The function of this second hydrophobic core may simply be stabilization of helix B, since removal of helices C through E leads to unfolding of the distal part of helix B and binding of the unwound element into the substrate-binding pocket (Jiang et al., 2005; Wang et al., 1998). So far, only the high-affinity conformation of the SBD is well defined. Peptides are bound in an extended conformation stabilized by several hydrogen bonds between the SBD and peptide backbone of the substrate and by hydrophobic interactions between a single substrate residue that reaches into a deep hydrophobic pocket of the SBD. Hydrophobic contacts between substrate residues and SBD residues that form an arch over the substrate backbone stabilize the Hsp70-peptide complex further.

This arrangement makes it clear that peptide binding and release require substantial conformational changes in the SBD. Substrate cannot enter or be released from the ADP state without increasing the distance between the distal part of helix B and the outer loops and the opening of the arch over the peptide backbone. Since substrate association and dissociation rates are appreciable in the high-affinity state, spontaneous opening and closing of the substrate-binding pocket must occur in this state (Mayer et al., 2000). Opening of the substrate-binding pocket must be even more prominent in the ATP-bound state, since this state displays 100- and 1000-fold higher peptide association and dissociation rates.

Based on crystallographic data, Hendrickson and coworkers proposed that helix B melts around a central hinge region, allowing helices C through E to swing upward and the outer loops to become more flexible, thereby opening a path to the substrate-binding pocket (Zhu et al., 1996). The recently elucidated Hsp110 structure has been proposed to model the Hsp70 ATP state structure and suggests a conformation with helix B completely detached from the β sheet subdomain and swung upward to form a continuous helix with helix A (Figure 3C) (Liu and Hendrickson, 2007). Although the degree of sequence identity between Hsp70 and Hsp110 proteins is low in the SBD, the subdomain structures of their respective SBDs are very similar, and mutational analyses suggest similar interdomain interfaces in both classes of proteins (Liu and Hendrickson, 2007). An NMR structure of the isolated β sheet domain

illustrates that such a complete removal of the helical lid would increase the conformational flexibility of the substrate-enclosing loops significantly (Figure 3B).

HX-MS experiments elucidated the differences in dynamics between the high- and the low-affinity conformations (Rist et al., 2006). In the nucleotide-free state, the distal part of helix B is in a folding-unfolding equilibrium that supports the hypothesis of helix B melting as the mechanism for substrate dissociation in the high-affinity state. However, in the ATP-bound state, melting of helix B was too slow to explain the increased rates of substrate release. Instead, a significant increase in flexibility was also observed in the inner loops of the SBD (Figure 3B), supporting a complete swinging upward of helix B, similar to the Hsp110 structure, which therefore may be close to the low-affinity conformation of Hsp70s.

Conformational Flexibility of the NBD

The NBD consists of two lobes with a deep cleft between them, at the bottom of which nucleotide binds. The lobes are subdivided into two subdomains each (Figure 3B). The various crystal structures of wild-type and mutant Hsp70 NBDs in the absence and presence of different nucleotides are highly similar, suggesting that the NBD is a rather static domain (Flaherty et al., 1990). The dynamic character of the NBD first became apparent from crystal structures in the presence of nucleotide exchange factors (Harrison et al., 1997; Polier et al., 2008; Schuermann et al., 2008; Shomura et al., 2005; Sondermann et al., 2001). Hsp70s interact with four different families of nucleotide exchange factors: the GrpE family in prokaryotes and organelles of prokaryotic origin, the Bag family in the eukaryotic cytosol, the HspBP family in the eukaryotic cytosol and endoplasmic reticulum, and the Hsp70-related Hsp110 and Hsp170 proteins in the eukaryotic cytosol (Hsp110) and endoplasmic reticulum (Hsp170). Three of these families (GrpE, Bag, and Hsp110/Hsp170) induce a similar 14° outward rotation of subdomain IIB, while HspBP1 clasps subdomain IIB and thereby apparently pushes subdomain IB out of plane and destabilizes its structure (Figure 3D). NMR residual dipolar coupling experiments showed that shearing and tilting movements of the NBD subdomains also exist in the absence of nucleotide exchange factors (Figure 3) (Bhattacharya et al., 2009; Woo et al., 2009; Zhang and Zuiderweg, 2004). These conformational oscillations of the subdomains are influenced by binding of nucleotide, as suggested by the fact that nucleotide is coordinated by residues from all four subdomains and demonstrated by HX-MS experiments, which found a general stabilization of all parts of the NBD upon nucleotide binding (Bhattacharya et al., 2009; Rist et al., 2006; Woo et al., 2009). The relative subdomain movements, which affect basal nucleotide exchange rates, seem to vary significantly within the family of Hsp70 proteins, as inferred from the large differences in basal nucleotide dissociation rates (Brehmer et al., 2001).

Allosteric Coupling of the Two Domains

ATP binding to the NBD increases substrate dissociation rates by three orders of magnitude, and binding of substrate and a J-domain protein stimulates the ATPase rate by 2–3 orders of magnitude. Thus, the conformation of the NBD and SBD are allosterically coupled. The mechanism of this coupling is still poorly understood. In the nucleotide-free state, the NBD and SBD do not seem to have extensive interactions (Bertelsen et al., 2009). Upon ATP binding, both domains seem to dock in a conformation that may be similar to the Hsp110 structure. However, since Hsp110 proteins exhibit no allosteric coupling between the NBD and SBD, the Hsp110 structure gives no insights into the allosteric coupling mechanism of the Hsp70s. Conformational changes in the NBD are transduced to the SBD through the conserved linker, which becomes protected from hydrogen exchange upon ATP binding (Rist et al., 2006; Vogel et al., 2006a). The linker is also critical for triggering ATP hydrolysis upon substrate binding (Vogel et al., 2006b). The linker may also be involved in the transduction of the ATPase-stimulating signal from the J-domain (Jiang et al., 2007).

Role of ATP Hydrolysis and Effects on Substrates

How are the conformational changes in the NBD and SBD and allosteric communication between the domains linked to the chaperone activity of Hsp70s? Coupling of ATP hydrolysis to substrate binding allows rapid substrate association to the ATP state and slow dissociation from the ADP state. This conformational cycle increases the apparent affinity of Hsp70 for substrates by two orders of magnitude as compared to the high-affinity ADP conformation alone. In addition, it has been proposed that the ATPase cycle of Hsp70s is linked to conformational changes that can act as a pulling force to unfold translocating polypeptides during import into mitochondria or the endoplasmic reticulum (Matouschek et al., 2000). Since NBD and SBD are docked in the ATP-bound state and lose most tight contacts in the ADP-bound state, such pulling could be directly coupled to γ-phosphate cleavage. Direct structural evidence for force generation by Hsp70s through conformational changes is still missing.

In addition, the conformation of substrates can be affected by the binding of Hsp70s, as demonstrated recently by HX-MS (Rodriguez et al., 2008). When the *E. coli* heat shock transcription factor σ^{32} is bound to *E. coli* Hsp70 DnaK, a defined region exhibits local unfolding. When the J-domain cochaperone DnaJ was bound to σ^{32} in the absence of DnaK, different parts of σ^{32} were unfolded, indicating that protein binding alone, even without ATP hydrolysis, can shift the equilibrium of the bound protein to a more unfolded state. Whether the chaperones induce the unfolding or trap a more unfolded state from a conformational equilibrium is not clear. Since σ^{32} is a native protein substrate of DnaK and may therefore be a special case, it is unclear whether local unfolding is operational for refolding of misfolded proteins.

Hsp90: Nucleotide-Controlled Conformational Equilibria

Hsp90s, like Hsp60s and Hsp70s, can bind to misfolded proteins and prevent their aggregation. However, their main—and in all eukaryotic cells, essential—function is believed to be the interaction with a defined set of proteins, called clients, in a native or near-native state. Many of these clients are transcription factors and protein kinases involved in the control of cell homeostasis, proliferation, differentiation, and apoptosis (Pearl and Prodromou, 2006; Richter and Buchner, 2006).

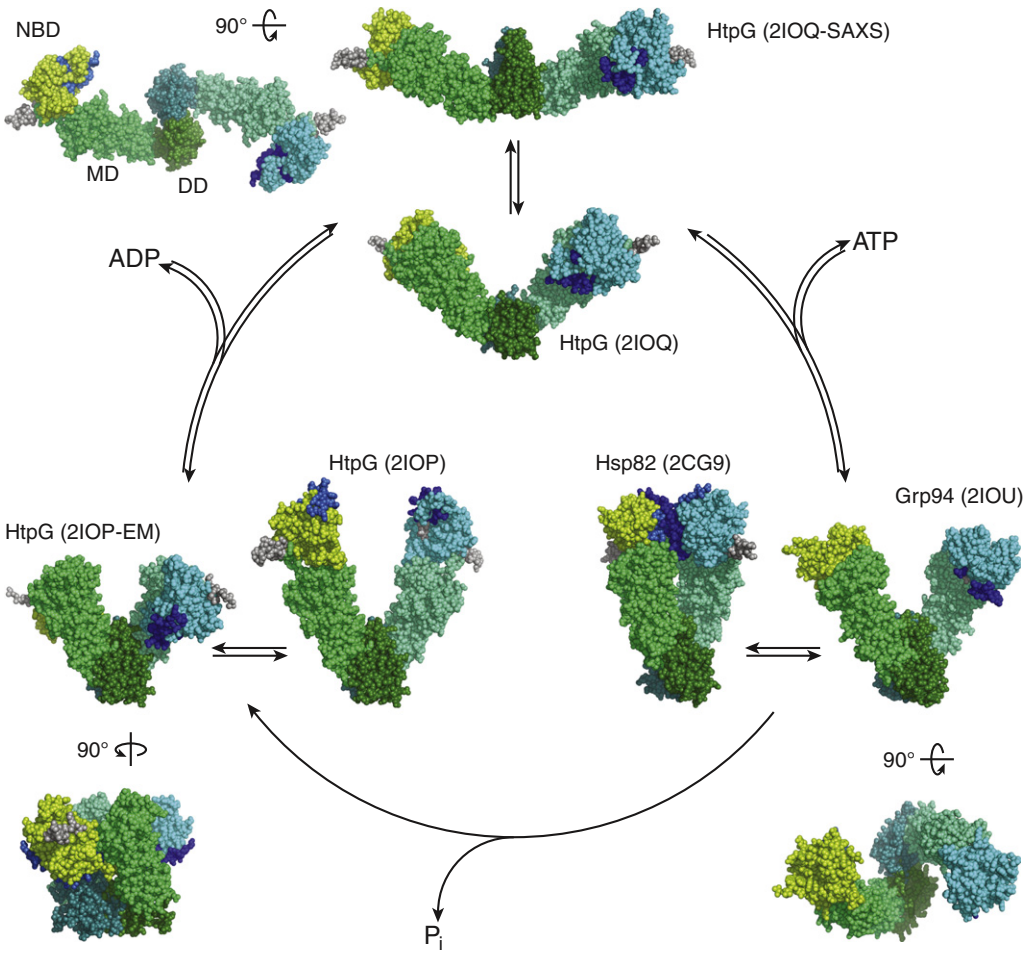

Figure 4. Conformational Equilibria in Hsp90s
Sphere representation of crystal structures of different Hsp90 proteins (PDB entry codes as indicated) and models derived from negative stain EM and SAXS. Residues of the NBD, which are in the interface upon N-terminal dimerization, are colored in blue. In gray are residues of the charged linker between NBD and MD. PDB files for the models derived by EM and SAXS data were kindly provided by D. Agard.

Hsp90 proteins consist of three functional domains: the N-terminal NBD; the middle domain (MD), which is involved in ATP hydrolysis and client and cochaperone binding; and a C-terminal dimerization domain (DD). A functional chaperone cycle for Hsp90s was first proposed on the basis of their interaction with steroid hormone receptors (reviewed in Picard, 2006). Steroid hormone receptors first interact with Hsp70 in an ATP-dependent and Hsp40-catalyzed reaction. The dimeric cochaperone Hop binds to Hsp70 and Hsp90, thereby stabilizing an early client-Hsp90 complex. The cochaperone p23 and peptidyl-prolyl-*cis*/*trans*-isomerases displace Hop and Hsp70, leading to the mature complex. Kinases depend on Cdc37 for their interaction with Hsp90s. The Hsp90-client complex is believed to decay with a half-life of 5 min, and the client re-enters the cycle by binding to Hsp40 and Hsp70.

The ATPase Cycle: A Conformational Dance

The crystal structures of full-length Hsp90 proteins from three different species in the absence of nucleotides and in the presence of ADP or AMPNP revealed highly similar domain structures but significant differences in the orientation of the domains relative to each other (Figure 4) (Ali et al., 2006; Dollins et al., 2007; Shiau et al., 2006). These structures, together with negative stain EM and SAXS data, indicated that Hsp90 proteins have a large degree of conformational freedom ranging from a wide open V-shaped conformation with the protomers only contacting each other in the DD to an intertwined conformation with additional close contacts between the two NBDs in the Hsp90 dimer (Krukenberg et al., 2008). Furthermore, the NBDs appear to be able to rotate freely around the longitudinal axis of the molecule and an axis perpendicular to it.

The only well-defined conformation is the domain arrangement necessary for ATP hydrolysis. In this conformation, the two Hsp90 protomers are twisted around each other with close contact between the two NBDs and between NBDs and MDs. The necessity of NBD dimerization for ATP hydrolysis was deduced earlier from the structural similarity of Hsp90 with MutL and Gyrase B and biochemical data (Prodromou et al., 1997, 2000; Richter et al., 2001).

Buchner and coworkers recently analyzed the kinetics of N-terminal dimerization (Hessling et al., 2009). They labeled the NBD or MD with different dyes and mixed Hsp90 proteins in various combinations to allow use of FRET as a measure for the distance between these domains. FRET increased upon addition of the nonhydrolyzable ATP analog ATPγS, indicating that the N-domains approached each other and the dimer conformation was arrested in the closed conformation. Such a change in distance was not observed in the presence of ATP, suggesting that the closed conformation is very transient. Analysis of the FRET kinetics demonstrated that the ATP-bound state consists of an ensemble of different conformations, with the open conformation being most prevalent. A similar conclusion came of an EM study of three Hsp90 proteins from bacteria, yeast, and humans (Southworth and Agard, 2008). Open and closed conformations were found in all different proteins in the apo, ADP, and AMPPNP states. Interestingly, the relative abundance of the different states varied between the three proteins, explaining the different ATP hydrolysis rates. Agard and coworkers presented evidence for an additional, highly compact conformation of *E. coli* Hsp90 in the presence of ADP, with the NBD packed against the upper half of both MDs in the dimer (Shiau et al., 2006; Southworth and Agard, 2008) (Figure 4). Such a compact conformation is proposed to represent the posthydrolysis state that dissociates substrates by displacing them from hydrophobic surface areas (Shiau et al., 2006). This state was not detectable by SAXS and HX-MS experiments, indicating that it could be only a minor species in the conformational ensemble (Graf et al., 2009; Krukenberg et al., 2008).

The domain dynamics of the yeast Hsp90 was most impressively demonstrated by single-molecule FRET experiments by Hugel and coworkers (Mickler et al., 2009). The analysis of the FRET kinetics revealed that in all states of the ATPase cycle—the apo, ATP, and ADP states—Hsp90 continuously fluctuates between two closed and two open conformations. The difference between the nucleotide states is due to different forward and back transition rates.

This domain "belly dance" is not simply restricted to rigid body movements, as originally proposed, but involves high secondary structure flexibility, as revealed by two HX-MS studies (Graf et al., 2009; Phillips et al., 2007). Interestingly, addition of ATP, but not ADP, induced a high degree of protection from hydrogen exchange in *E. coli* HtpG, which seems at odds with the continuous opening and closing shown for yeast Hsp90. In addition, the transition from the relaxed apo state to the tensed ATP state was rather slow, with a half-life of about 2 min, and involved a stepwise transition starting at the nucleotide-binding pocket and progressing through the molecule to the N terminus and the MD (Graf et al., 2009).

Regulation of the Conformational States

Four cochaperones were shown to influence the conformational dynamics of eukaryotic Hsp90 proteins. Hop/Sti1 inhibits ATP hydrolysis by stabilizing the open conformation, as revealed by FRET experiments (Hessling et al., 2009). Structural details for this action of Hop/Sti1 are still elusive, since its primary interaction site is the C-terminal MEEVD motif. Cdc37 also inhibits ATP hydrolysis by stabilizing an open conformation. Crystallographic and cryo-EM data suggest that it binds to the NBD and thus prevents N-terminal dimerization (Roe et al., 2004; Vaughan et al., 2006). p23/Sba1 binds stably to the ATP-bound closed conformation and stabilizes Hsp90 in a hydrolysis-competent conformation (Ali et al., 2006). However, it is not clear how it inhibits ATP hydrolysis. Aha1 stabilizes Hsp90 in a similar ATP hydrolysis-competent conformation and accelerates γ-phosphate cleavage (Meyer et al., 2004). Interestingly, Aha1 binding to one Hsp90 subunit is sufficient to induce conformational changes, resulting in an asymmetric complex (Retzlaff et al., 2010). Aha1 binding restricts some intermediate conformations and thus accelerates the transition to the closed conformation (Hessling et al., 2009).

Posttranslational modifications also regulate the conformational flexibility of Hsp90 proteins. S-nitrosylation of a cysteine located between the MD and DD of human Hsp90 dramatically reduces the ATPase activity by altering the rate of N-terminal dimerization (Retzlaff et al., 2009). The recently discovered phosphorylation of a tyrosine in the NBD of yeast and human Hsp90 also seems to reduce N-terminal dimerization and ATPase activity (Mollapour et al., 2010). Several other sites for phosphorylation and acetylation are located in the hinge regions between the NBD and MD and the MD and DD of Hsp90, which would be expected to alter domain movement in addition to the effects on local conformational flexibility.

Conformational Dynamics and Client Interaction

It is still rather unclear how domain movements and conformational flexibility affect the interaction with clients and how they influence client conformation. Binding of many clients to Hsp90 requires or is at least accelerated by the cochaperones Hop/Sti1 and Cdc37, which are known to stabilize the open conformation (Arlander et al., 2006; Morishima et al., 2000). ATP hydrolysis and N-terminal dimerization are essential in vivo and were shown to accelerate client release (Obermann et al., 1998; Panaretou et al., 1998; Young and Hartl, 2000). The cochaperone p23/Sba1, which stabilizes a closed, prehydrolysis conformation, also enhances activation of some client proteins, notably steroid hormone receptors (Morishima et al., 2003). Phosphorylation of an N-terminal tyrosine, which is supposed to slow down if not prevent N-terminal dimerization, significantly enhances the inhibitory effect of Hsp90 on the heat shock transcription factor (Mollapour et al., 2010). The ATPase-stimulating cochaperone Aha1 also enhances activation of client proteins (Panaretou et al., 2002). Together, these data suggest that clients associate with an open conformer of Hsp90, and subsequent closing and N-terminal dimerization is necessary for client activation and release. Whether such a domain movement exerts conformational strains on the client is unknown.

Hsp100: Harnessing ATP Hydrolysis to Generate Movement

The Hsp100/Clp family of chaperones belongs to the superfamily of AAA+ domain-containing *A*TPases *a*ssociated with various cellular *a*ctivities (Tucker and Sallai, 2007). The AAA+ domain is characterized by the Walker A, Walker B, sensor 1, and sensor 2 sequence motifs and consists of two subdomains: the large

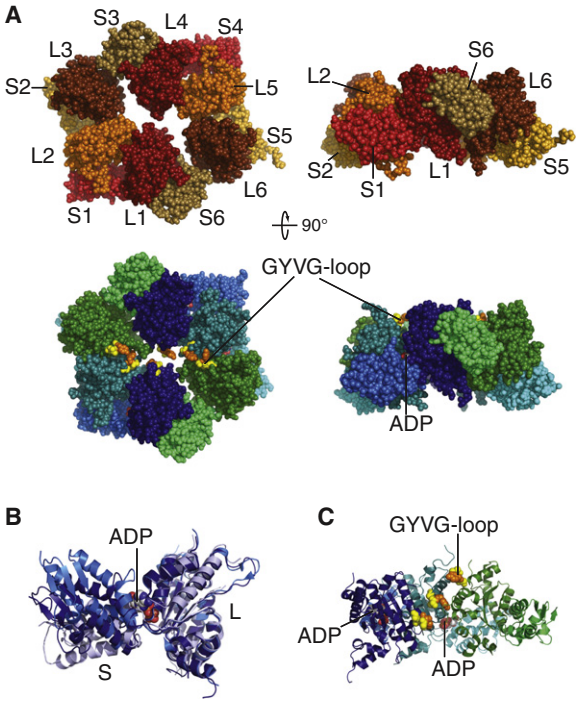

Figure 5. Structure of N-Terminally Deleted ClpX

(A) Sphere representation of the crystal structure of the nucleotide-free (upper panels) and ADP-bound (lower panels) ClpX pseudohexamer (PDB entry codes 3HTE and 3HWS), with large AAA+ subdomain (L1– L6) in dark colors and small AAA+ subdomains (S1–S6) in corresponding lighter colors. The substrate-interacting GYVG loop is colored in yellow with the tyrosine in orange.

(B) Secondary structure representation of an overlay of the first three subunits (dark blue, marine, light blue) of the pseudohexameric ClpX aligned in the large subunits.

(C) Secondary structure representation of subunits 1–3 of the ClpX pseudohexamer in the presence of ADP colored as in (A), lower panel. The substrate-interacting GYVG loop is colored in yellow with the tyrosine in orange.

αβ-subdomain, built of a five-stranded parallel β sheet with two α helices on one side and three on the other, and the small α-subdomain with four α helices. Most AAA+ proteins form oligomers with ATP bound close to the interface between subunits, and the neighboring subunit contributes the so-called arginine finger for ATP hydrolysis. Hsp100 proteins contain one or two AAA+ domains arranged in hexameric rings with a central pore through which substrate proteins can be threaded. Many Hsp100 proteins (ClpA, ClpX, HslU in *E. coli*) associate with ring-forming peptidases (ClpP, HslV), unfold proteins, and feed them into the proteolytic chamber. ClpB in *E. coli* and its relatives in lower eukaryots (Hsp104) and plants (Hsp101) do not associate with peptidases but cooperate with the Hsp70 system to dissolve protein aggregates.

The ATPase Cycle

The molecular mechanism of Hsp100 chaperones is best understood for ClpX due to elegant work from the Sauer lab. They created covalently linked ClpX-pseudohexamers, allowing the specific introduction of mutations in individual subunits (Martin et al., 2005). Two crystal structures of this covalently linked ClpX protein provide key insights into the conformational changes associated with the ATPase cycle and suggest a mechanism by which ATP hydrolysis is coupled to substrate translocation (Glynn et al., 2009). In the presence of ADP, ClpX crystallized as an asymmetric hexamer with two types of subunits in a 1-1-2-1-1-2 arrangement (Figure 5). ADP is bound at the 1-1 and the 1-2 interfaces, but not at the 2-1 interfaces, resulting in four molecules ADP bound per hexamer. The small subdomain of the AAA+ domain is tightly associated with the large subdomain of the neighboring subunit, forming a functional entity that seems to move like a rigid body around swivel points. These entities are staggered with respect to the central pore axis, affecting the position of loops that were shown to be important for substrate translocation (Martin et al., 2008). Surprisingly, in the absence of nucleotide, ClpX crystallized in a similar asymmetric assembly, with subunits in nucleotide binding-competent conformations and subunits in a state seemingly incompetent for nucleotide binding. Interestingly, the central pore is much wider in the nucleotide-free form of ClpX. This indicates that (1) the asymmetry is an inherent feature of ClpX and not induced by nucleotide binding and (2) the width of the central opening is not fixed, but can be adjusted as needed for a tight grip on a polypeptide chain in the process of unfolding or to get a hold onto a bulky substrate. The following picture emerges from these structures and a large body of biochemical data. Nucleotide association to a binding-competent subunit leads to a rotation between the large and small AAA+ subdomains and with it the large subdomain of the neighboring subunit. This movement is propagated to the third subunit, leading to different positions of the central substrate-binding GYVG loop, which is close to the bottom of the pore in the first subunit, in a middle position in the second subunit, and in an up position in the third subunit. A second loop (pore 2 loop) that seems to be important for preventing back-sliding of the substrate is also in different positions (Figure 5). As ClpX progresses through the ATPase cycle, different subunits interact with their GYVG loop in the up position with the substrate polypeptide and, upon ATP binding and hydrolysis, perform a rolling movement, which brings the loop into the down position. The asymmetric assembly of ClpX illustrates clearly that the subunits cannot act in a concerted fashion. Biochemical data suggest that the subunits also do not act sequentially and more likely work by a random stroke mechanism (Martin et al., 2005).

A similar mechanism seems to be operational for the Hsp100 chaperones with two AAA+ domains per subunit (NBD1 and NBD2) arranged in a double ring. Substrate threading was demonstrated for ClpB and Hsp104, which do not interact with a peptidase but with the Hsp70 chaperone system in solubilization of protein aggregates (Tessarz et al., 2008; Weibezahn et al., 2004). Essential for this substrate threading are two tyrosine-containing loops, one in each AAA+ domain. Cryo-EM reconstructions of an Hsp104 variant, which could not hydrolyze ATP in NBD2, in different nucleotide states indicate large movements in each AAA+ domain, up to 90° within the plane of the ring and up to 60° parallel to the central pore (Wendler et al., 2009) (Figure 6). However, no indications were found that a domain swap, as observed in ClpX with the small AAA+

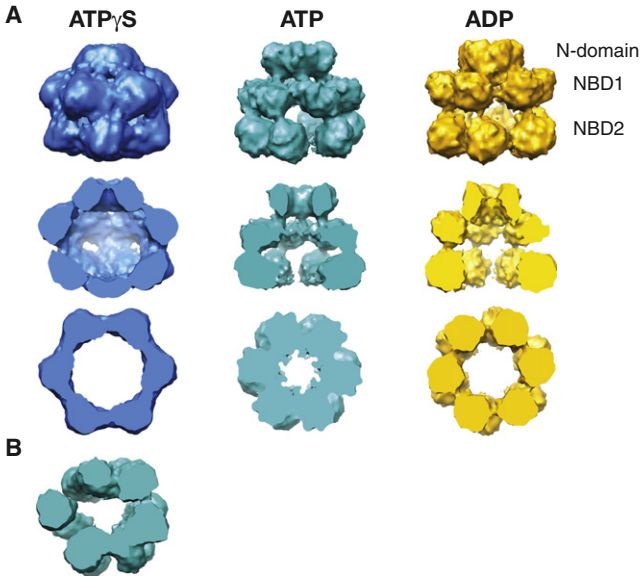

Figure 6. Conformational Changes in Yeast Hsp104
(A) Cryo-EM reconstructions with six-fold symmetry of an Hsp104 variant deficient in ATP hydrolysis in NBD2 (Hsp104-N728A) in the presence of ATPγS, ATP, and ADP. Upper panels, side view; middle panel, cut-open side view; lower panel, cross-section through NBD1.
(B) Cross-section through NBD1 of an asymmetric cryo-EM reconstruction of Hsp104-N728A in the presence of ATP.

subdomain of one subunit interacting with the large AAA+ subdomain of the neighboring subunit, also occurs in Hsp104. If ATP is bound to NBD2 and ADP to NBD1, the tyrosine loop of NBD1 is in a down position, close to the interface of the two rings, and the tyrosine loop of NBD2 is in an up position, ready to interact with substrates. ATP binding to NBD1 leads to an upward rotation of NBD1 and, concomitantly, to a downward rotation of NBD2 that is proposed to exert the power stroke that extracts polypeptides from protein aggregates. ATP hydrolysis in NBD1 rotates the domain downward toward a neighboring subunit and is suggested to pull the substrate into the Hsp104 cavity. Asymmetric reconstructions of the EM images suggest that ATP binding and hydrolysis occur in a sequential manner in the NBD1 ring. Whether the Hsp104 homolog ClpB works in a similar way is currently unclear, since cryo-EM images of ClpB show significantly different conformations (Lee et al., 2007).

Outlook

Much progress has been made in understanding the molecular gymnastics of the different chaperones. Not only is the diversity of conformational changes of these molecular chaperones astounding, but also the different uses of ATP hydrolysis: as timer (Hsp60), to increase affinity through nonequilibrium binding (Hsp70), to switch between different conformational equilibria (Hsp90), and for force generation (Hsp100). Concerning the molecular mechanism of the chaperones, a clear picture is emerging for Hsp60s and Hsp100s, though substrate binding and the early events of folding (Hsp60) and unfolding (Hsp100) are still debated. For Hsp100s, it is also unclear how stalled substrates are dealt with and whether dissociation of the hexamer is an option or even part of the mechanism. The picture is less clear for Hsp70s and Hsp90s. The large conformational space sampled by Hsp90s is puzzling but may be necessary to accommodate all the different substrates that are not related in sequence or structure. Cochaperones and posttranslational modifications appear to program the conformation of Hsp90 for specific substrates. For Hsp70s, it is still unclear at a structural level how the two domains interact and communicate with each other, how J-domain proteins stimulate Hsp70s' ATPase activity, and how binding and release by Hsp70s assist refolding of denatured proteins. The molecular mechanism of the cooperation of Hsp70s with Hsp90 in client protein activation and with Hsp100 in protein disaggregation provides a further major challenge for the future.

The ability of chaperones to assist de novo folding, to refold misfolded proteins, and to counteract protein aggregation paved the way for more flexibility in proteins and for larger proteins with many domains. Therefore, chaperones may have been a significant driving force in the evolution of complex protein functions.

ACKNOWLEDGMENTS

I thank D. Agard for providing the PDB files of his models of HtpG and E. Deuerling, S. Rüdiger, and K. Turgay for their helpful comments on the manuscript. I am also in debt to the anonymous reviewer for his/her extensive editorial comments on the manuscript. My apologies to the many researchers who have contributed tremendously to the understanding of the mechanism of chaperones, but whose work I could not cite due to space limitations. The work of the author on Hsp70 and Hsp90 is funded by the Deutsche Forschungsgemeinschaft (SFB638, TRR77).

REFERENCES

Ali, M.M., Roe, S.M., Vaughan, C.K., Meyer, P., Panaretou, B., Piper, P.W., Prodromou, C., and Pearl, L.H. (2006). Crystal structure of an Hsp90-nucleotide-p23/Sba1 closed chaperone complex. Nature *440*, 1013–1017.

Arlander, S.J., Felts, S.J., Wagner, J.M., Stensgard, B., Toft, D.O., and Karnitz, L.M. (2006). Chaperoning checkpoint kinase 1 (Chk1), an Hsp90 client, with purified chaperones. J. Biol. Chem. *281*, 2989–2998.

Bertelsen, E.B., Chang, L., Gestwicki, J.E., and Zuiderweg, E.R. (2009). Solution conformation of wild-type E. coli Hsp70 (DnaK) chaperone complexed with ADP and substrate. Proc. Natl. Acad. Sci. USA *106*, 8471–8476.

Bhattacharya, A., Kurochkin, A.V., Yip, G.N., Zhang, Y., Bertelsen, E.B., and Zuiderweg, E.R. (2009). Allostery in Hsp70 chaperones is transduced by subdomain rotations. J. Mol. Biol. *388*, 475–490.

Bigotti, M.G., and Clarke, A.R. (2005). Cooperativity in the thermosome. J. Mol. Biol. *348*, 13–26.

Booth, C.R., Meyer, A.S., Cong, Y., Topf, M., Sali, A., Ludtke, S.J., Chiu, W., and Frydman, J. (2008). Mechanism of lid closure in the eukaryotic chaperonin TRiC/CCT. Nat. Struct. Mol. Biol. *15*, 746–753.

Braig, K., Otwinowski, Z., Hegde, R., Boisvert, D.C., Joachimiak, A., Horwich, A.L., and Sigler, P.B. (1994). The crystal structure of the bacterial chaperonin GroEL at 2.8 A. Nature *371*, 578–586.

Brehmer, D., Rüdiger, S., Gässler, C.S., Klostermeier, D., Packschies, L., Reinstein, J., Mayer, M.P., and Bukau, B. (2001). Tuning of chaperone activity of Hsp70 proteins by modulation of nucleotide exchange. Nat. Struct. Biol. *8*, 427–432.

Clare, D.K., Stagg, S., Quispe, J., Farr, G.W., Horwich, A.L., and Saibil, H.R. (2008). Multiple states of a nucleotide-bound group 2 chaperonin. Structure *16*, 528–534.

Dollins, D.E., Warren, J.J., Immormino, R.M., and Gewirth, D.T. (2007). Structures of GRP94-nucleotide complexes reveal mechanistic differences between the hsp90 chaperones. Mol. Cell *28*, 41–56.

Flaherty, K.M., DeLuca-Flaherty, C., and McKay, D.B. (1990). Three-dimensional structure of the ATPase fragment of a 70K heat-shock cognate protein. Nature *346*, 623–628.

Franzmann, T.M., Menhorn, P., Walter, S., and Buchner, J. (2008). Activation of the chaperone Hsp26 is controlled by the rearrangement of its thermosensor domain. Mol. Cell *29*, 207–216.

Frydman, J. (2001). Folding of newly translated proteins in vivo: the role of molecular chaperones. Annu. Rev. Biochem. *70*, 603–647.

Glynn, S.E., Martin, A., Nager, A.R., Baker, T.A., and Sauer, R.T. (2009). Structures of asymmetric ClpX hexamers reveal nucleotide-dependent motions in a AAA+ protein-unfolding machine. Cell *139*, 744–756.

Graf, C., Stankiewicz, M., Kramer, G., and Mayer, M.P. (2009). Spatially and kinetically resolved changes in the conformational dynamics of the Hsp90 chaperone machine. EMBO J. *28*, 602–613.

Gutsche, I., Essen, L.-O., and Baumeister, W. (1999). Group II chaperonins: new TRiC(k)s and turns of a protein folding machine. J. Mol. Biol. *293*, 295–312.

Harrison, C.J., Hayer-Hartl, M., Di Liberto, M., Hartl, F.-U., and Kuriyan, J. (1997). Crystal structure of the nucleotide exchange factor GrpE bound to the ATPase domain of the molecular chaperone DnaK. Science *276*, 431–435.

Hartl, F.U., and Hayer-Hartl, M. (2009). Converging concepts of protein folding in vitro and in vivo. Nat. Struct. Mol. Biol. *16*, 574–581.

Henzler-Wildman, K., and Kern, D. (2007). Dynamic personalities of proteins. Nature *450*, 964–972.

Hessling, M., Richter, K., and Buchner, J. (2009). Dissection of the ATP-induced conformational cycle of the molecular chaperone Hsp90. Nat. Struct. Mol. Biol. *16*, 287–293.

Horwich, A.L., Fenton, W.A., Chapman, E., and Farr, G.W. (2007). Two families of chaperonin: physiology and mechanism. Annu. Rev. Cell Dev. Biol. *23*, 115–145.

Horwich, A.L., Apetri, A.C., and Fenton, W.A. (2009). The GroEL/GroES cis cavity as a passive anti-aggregation device. FEBS Lett. *583*, 2654–2662.

Janda, I., Devedjiev, Y., Derewenda, U., Dauter, Z., Bielnicki, J., Cooper, D.R., Graf, P.C., Joachimiak, A., Jakob, U., and Derewenda, Z.S. (2004). The crystal structure of the reduced, Zn2+-bound form of the B. subtilis Hsp33 chaperone and its implications for the activation mechanism. Structure *12*, 1901–1907.

Jiang, J., Prasad, K., Lafer, E.M., and Sousa, R. (2005). Structural basis of interdomain communication in the Hsc70 chaperone. Mol. Cell *20*, 513–524.

Jiang, J., Maes, E.G., Taylor, A.B., Wang, L., Hinck, A.P., Lafer, E.M., and Sousa, R. (2007). Structural basis of J cochaperone binding and regulation of Hsp70. Mol. Cell *28*, 422–433.

Kafri, G., Willison, K.R., and Horovitz, A. (2001). Nested allosteric interactions in the cytoplasmic chaperonin containing TCP-1. Protein Sci. *10*, 445–449.

Krukenberg, K.A., Förster, F., Rice, L.M., Sali, A., and Agard, D.A. (2008). Multiple conformations of E. coli Hsp90 in solution: insights into the conformational dynamics of Hsp90. Structure *16*, 755–765.

Lee, S., Choi, J.M., and Tsai, F.T. (2007). Visualizing the ATPase cycle in a protein disaggregating machine: structural basis for substrate binding by ClpB. Mol. Cell *25*, 261–271.

Lin, Z., and Rye, H.S. (2004). Expansion and compression of a protein folding intermediate by GroEL. Mol. Cell *16*, 23–34.

Lin, Z., Madan, D., and Rye, H.S. (2008). GroEL stimulates protein folding through forced unfolding. Nat. Struct. Mol. Biol. *15*, 303–311.

Liu, Q., and Hendrickson, W.A. (2007). Insights into Hsp70 chaperone activity from a crystal structure of the yeast Hsp110 Sse1. Cell *131*, 106–120.

Martin, A., Baker, T.A., and Sauer, R.T. (2005). Rebuilt AAA + motors reveal operating principles for ATP-fuelled machines. Nature *437*, 1115–1120.

Martin, A., Baker, T.A., and Sauer, R.T. (2008). Pore loops of the AAA+ ClpX machine grip substrates to drive translocation and unfolding. Nat. Struct. Mol. Biol. *15*, 1147–1151.

Matouschek, A., Pfanner, N., and Voos, W. (2000). Protein unfolding by mitochondria. The Hsp70 import motor. EMBO Rep. *1*, 404–410.

Mayer, M.P., and Bukau, B. (2005). Hsp70 chaperones: cellular functions and molecular mechanism. Cell. Mol. Life Sci. *62*, 670–684.

Mayer, M.P., Rüdiger, S., and Bukau, B. (2000). Molecular basis for interactions of the DnaK chaperone with substrates. Biol. Chem. *381*, 877–885.

Meimaridou, E., Gooljar, S.B., and Chapple, J.P. (2009). From hatching to dispatching: the multiple cellular roles of the Hsp70 molecular chaperone machinery. J. Mol. Endocrinol. *42*, 1–9.

Meyer, A.S., Gillespie, J.R., Walther, D., Millet, I.S., Doniach, S., and Frydman, J. (2003). Closing the folding chamber of the eukaryotic chaperonin requires the transition state of ATP hydrolysis. Cell *113*, 369–381.

Meyer, P., Prodromou, C., Liao, C., Hu, B., Roe, S.M., Vaughan, C.K., Vlasic, I., Panaretou, B., Piper, P.W., and Pearl, L.H. (2004). Structural basis for recruitment of the ATPase activator Aha1 to the Hsp90 chaperone machinery. EMBO J. *23*, 1402–1410.

Mickler, M., Hessling, M., Ratzke, C., Buchner, J., and Hugel, T. (2009). The large conformational changes of Hsp90 are only weakly coupled to ATP hydrolysis. Nat. Struct. Mol. Biol. *16*, 281–286.

Mollapour, M., Tsutsumi, S., Donnelly, A.C., Beebe, K., Tokita, M.J., Lee, M.J., Lee, S., Morra, G., Bourboulia, D., Scroggins, B.T., et al. (2010). Swe1Wee1-dependent tyrosine phosphorylation of Hsp90 regulates distinct facets of chaperone function. Mol. Cell *37*, 333–343.

Morishima, Y., Kanelakis, K.C., Silverstein, A.M., Dittmar, K.D., Estrada, L., and Pratt, W.B. (2000). The Hsp organizer protein hop enhances the rate of but is not essential for glucocorticoid receptor folding by the multiprotein Hsp90-based chaperone system. J. Biol. Chem. *275*, 6894–6900.

Morishima, Y., Kanelakis, K.C., Murphy, P.J., Lowe, E.R., Jenkins, G.J., Osawa, Y., Sunahara, R.K., and Pratt, W.B. (2003). The hsp90 cochaperone p23 is the limiting component of the multiprotein hsp90/hsp70-based chaperone system in vivo where it acts to stabilize the client protein: hsp90 complex. J. Biol. Chem. *278*, 48754–48763.

Obermann, W.M., Sondermann, H., Russo, A.A., Pavletich, N.P., and Hartl, F.U. (1998). In vivo function of Hsp90 is dependent on ATP binding and ATP hydrolysis. J. Cell Biol. *143*, 901–910.

Panaretou, B., Prodromou, C., Roe, S.M., O'Brien, R., Ladbury, J.E., Piper, P.W., and Pearl, L.H. (1998). ATP binding and hydrolysis are essential to the function of the Hsp90 molecular chaperone *in vivo*. EMBO J. *17*, 4829–4836.

Panaretou, B., Siligardi, G., Meyer, P., Maloney, A., Sullivan, J.K., Singh, S., Millson, S.H., Clarke, P.A., Naaby-Hansen, S., Stein, R., et al. (2002). Activation of the ATPase activity of hsp90 by the stress-regulated cochaperone aha1. Mol. Cell *10*, 1307–1318.

Pearl, L.H., and Prodromou, C. (2006). Structure and mechanism of the Hsp90 molecular chaperone machinery. Annu. Rev. Biochem. *75*, 271–294.

Phillips, J.J., Yao, Z.P., Zhang, W., McLaughlin, S., Laue, E.D., Robinson, C.V., and Jackson, S.E. (2007). Conformational dynamics of the molecular chaperone Hsp90 in complexes with a co-chaperone and anticancer drugs. J. Mol. Biol. *372*, 1189–1203.

Picard, D. (2002). Heat-shock protein 90, a chaperone for folding and regulation. Cell. Mol. Life Sci. *59*, 1640–1648.

Picard, D. (2006). Chaperoning steroid hormone action. Trends Endocrinol. Metab. *17*, 229–235.

Polier, S., Dragovic, Z., Hartl, F.U., and Bracher, A. (2008). Structural basis for the cooperation of Hsp70 and Hsp110 chaperones in protein folding. Cell *133*, 1068–1079.

Prodromou, C., Roe, S.M., O'Brien, R., Ladbury, J.E., Piper, P.W., and Pearl, L.H. (1997). Identification and structural characterization of the ATP/ADP-binding site in the Hsp90 molecular chaperone. Cell *90*, 65–75.

Prodromou, C., Panaretou, B., Chohan, S., Siligardi, G., O'Brien, R., Ladbury, J.E., Roe, S.M., Piper, P.W., and Pearl, L.H. (2000). The ATPase cycle of Hsp90 drives a molecular 'clamp' via transient dimerization of the N-terminal domains. EMBO J. *19*, 4383–4392.

Ranson, N.A., Farr, G.W., Roseman, A.M., Gowen, B., Fenton, W.A., Horwich, A.L., and Saibil, H.R. (2001). ATP-bound states of GroEL captured by cryo-electron microscopy. Cell *107*, 869–879.

Ranson, N.A., Clare, D.K., Farr, G.W., Houldershaw, D., Horwich, A.L., and Saibil, H.R. (2006). Allosteric signaling of ATP hydrolysis in GroEL-GroES complexes. Nat. Struct. Mol. Biol. *13*, 147–152.

Retzlaff, M., Stahl, M., Eberl, H.C., Lagleder, S., Beck, J., Kessler, H., and Buchner, J. (2009). Hsp90 is regulated by a switch point in the C-terminal domain. EMBO Rep. *10*, 1147–1153.

Retzlaff, M., Hagn, F., Mitschke, L., Hessling, M., Gugel, F., Kessler, H., Richter, K., and Buchner, J. (2010). Asymmetric activation of the hsp90 dimer by its cochaperone aha1. Mol. Cell *37*, 344–354.

Richter, K., and Buchner, J. (2006). hsp90: twist and fold. Cell *127*, 251–253.

Richter, K., Muschler, P., Hainzl, O., and Buchner, J. (2001). Coordinated ATP hydrolysis by the Hsp90 dimer. J. Biol. Chem. *276*, 33689–33696.

Rist, W., Graf, C., Bukau, B., and Mayer, M.P. (2006). Amide hydrogen exchange reveals conformational changes in hsp70 chaperones important for allosteric regulation. J. Biol. Chem. *281*, 16493–16501.

Rodriguez, F., Arsène-Ploetze, F., Rist, W., Rüdiger, S., Schneider-Mergener, J., Mayer, M.P., and Bukau, B. (2008). Molecular basis for regulation of the heat shock transcription factor sigma32 by the DnaK and DnaJ chaperones. Mol. Cell *32*, 347–358.

Roe, S.M., Ali, M.M., Meyer, P., Vaughan, C.K., Panaretou, B., Piper, P.W., Prodromou, C., and Pearl, L.H. (2004). The Mechanism of Hsp90 regulation by the protein kinase-specific cochaperone p50(cdc37). Cell *116*, 87–98.

Schuermann, J.P., Jiang, J., Cuellar, J., Llorca, O., Wang, L., Gimenez, L.E., Jin, S., Taylor, A.B., Demeler, B., Morano, K.A., et al. (2008). Structure of the Hsp110:Hsc70 nucleotide exchange machine. Mol. Cell *31*, 232–243.

Sharma, S., Chakraborty, K., Müller, B.K., Astola, N., Tang, Y.C., Lamb, D.C., Hayer-Hartl, M., and Hartl, F.U. (2008). Monitoring protein conformation along the pathway of chaperonin-assisted folding. Cell *133*, 142–153.

Shiau, A.K., Harris, S.F., Southworth, D.R., and Agard, D.A. (2006). Structural Analysis of E. coli hsp90 reveals dramatic nucleotide-dependent conformational rearrangements. Cell *127*, 329–340.

Shomura, Y., Dragovic, Z., Chang, H.C., Tzvetkov, N., Young, J.C., Brodsky, J.L., Guerriero, V., Hartl, F.U., and Bracher, A. (2005). Regulation of Hsp70 function by HspBP1: structural analysis reveals an alternate mechanism for Hsp70 nucleotide exchange. Mol. Cell *17*, 367–379.

Shtilerman, M., Lorimer, G.H., and Englander, S.W. (1999). Chaperonin function: folding by forced unfolding. Science *284*, 822–825.

Sondermann, H., Scheufler, C., Schneider, C., Hohfeld, J., Hartl, F.U., and Moarefi, I. (2001). Structure of a Bag/Hsc70 complex: convergent functional evolution of Hsp70 nucleotide exchange factors. Science *291*, 1553–1557.

Southworth, D.R., and Agard, D.A. (2008). Species-dependent ensembles of conserved conformational states define the Hsp90 chaperone ATPase cycle. Mol. Cell *32*, 631–640.

Spiess, C., Meyer, A.S., Reissmann, S., and Frydman, J. (2004). Mechanism of the eukaryotic chaperonin: protein folding in the chamber of secrets. Trends Cell Biol. *14*, 598–604.

Tessarz, P., Mogk, A., and Bukau, B. (2008). Substrate threading through the central pore of the Hsp104 chaperone as a common mechanism for protein disaggregation and prion propagation. Mol. Microbiol. *68*, 87–97.

Tucker, P.A., and Sallai, L. (2007). The AAA+ superfamily—a myriad of motions. Curr. Opin. Struct. Biol. *17*, 641–652.

Vaughan, C.K., Gohlke, U., Sobott, F., Good, V.M., Ali, M.M., Prodromou, C., Robinson, C.V., Saibil, H.R., and Pearl, L.H. (2006). Structure of an Hsp90-Cdc37-Cdk4 complex. Mol. Cell *23*, 697–707.

Vogel, M., Bukau, B., and Mayer, M.P. (2006a). Allosteric regulation of Hsp70 chaperones by a proline switch. Mol. Cell *21*, 359–367.

Vogel, M., Mayer, M.P., and Bukau, B. (2006b). Allosteric regulation of Hsp70 chaperones involves a conserved interdomain linker. J. Biol. Chem. *281*, 38705–38711.

Wang, H., Kurochkin, A.V., Pang, Y., Hu, W., Flynn, G.C., and Zuiderweg, E.R.P. (1998). NMR solution structure of the 21 kDa chaperone protein DnaK substrate binding domain: a preview of chaperone-protein interaction. Biochemistry *37*, 7929–7940.

Weibezahn, J., Tessarz, P., Schlieker, C., Zahn, R., Maglica, Z., Lee, S., Zentgraf, H., Weber-Ban, E.U., Dougan, D.A., Tsai, F.T., et al. (2004). Thermotolerance requires refolding of aggregated proteins by substrate translocation through the central pore of ClpB. Cell *119*, 653–665.

Wendler, P., Shorter, J., Snead, D., Plisson, C., Clare, D.K., Lindquist, S., and Saibil, H.R. (2009). Motor mechanism for protein threading through Hsp104. Mol. Cell *34*, 81–92.

Woo, H.J., Jiang, J., Lafer, E.M., and Sousa, R. (2009). ATP-induced conformational changes in Hsp70: molecular dynamics and experimental validation of an in silico predicted conformation. Biochemistry *48*, 11470–11477.

Xu, Z., Horwich, A.L., and Sigler, P.B. (1997). The crystal structure of the asymmetric GroEL-GroES-(ADP)7 chaperonin complex. Nature *388*, 741–750.

Yifrach, O., and Horovitz, A. (1995). Nested cooperativity in the ATPase activity of the oligomeric chaperonin GroEL. Biochemistry *34*, 5303–5308.

Young, J.C., and Hartl, F.U. (2000). Polypeptide release by Hsp90 involves ATP hydrolysis and is enhanced by the co-chaperone p23. EMBO J. *19*, 5930–5940.

Zhang, Y., and Zuiderweg, E.R. (2004). The 70-kDa heat shock protein chaperone nucleotide-binding domain in solution unveiled as a molecular machine that can reorient its functional subdomains. Proc. Natl. Acad. Sci. USA *101*, 10272–10277.

Zhang, J., Baker, M.L., Schröder, G.F., Douglas, N.R., Reissmann, S., Jakana, J., Dougherty, M., Fu, C.J., Levitt, M., Ludtke, S.J., et al. (2010). Mechanism of folding chamber closure in a group II chaperonin. Nature *463*, 379–383.

Zhu, X., Zhao, X., Burkholder, W.F., Gragerov, A., Ogata, C.M., Gottesman, M.E., and Hendrickson, W.A. (1996). Structural analysis of substrate binding by the molecular chaperone DnaK. Science *272*, 1606–1614.